fermentation

MDPI

Article

Development of High Palmitoleic (16:1 n-7) Acid Oil by Fermentation of Microalgae

Xiaoying Zhou, Mona Correa, Dino Athanasiadis, Veronica Benites, Bryce Doherty, Lucy Edy, Christy Piamonte, Gener Eliares, Marvin Cornejo, Ting Gong, Leon Parker, Manuel Oliveira, Walter Rakitsky, James Casey Lippmeier, Jessica M. Walter and Frédéric Destaillats *

Checkerspot, Inc., Alameda, CA 94501, USA
* Correspondence: fdestaillats@checkerspot.com

Abstract

Palmitoleic acid (POA; 16:1 n-7 or *cis*-9 16:1) is a bioactive monounsaturated fatty acid (FA) with emerging metabolic and skin-health relevance, yet conventional botanical and animal sources provide limited and variable levels. Here we report on the development of a high-yield POA product platform in the heterotrophic microalga *Prototheca moriformis* through targeted genetic engineering. A Δ9-fatty acid desaturase from *Macadamia integrifolia* (*MiSAD1618*) was integrated using a phosphite-based selection system. Primary screening identified stable transformants producing up to 54% POA of total fatty acids, compared to 0.8% in the parental strain. In 1 L shake-flask cultivation, POA reached up to 58.2% of total fatty acids. In a 1 L fed-batch fermentation, the engineered strain accumulated 47.8 g/L of lipids with 43.5% POA after 96 h of fermentation, corresponding to 20.8 g/L of POA. GC–MS analysis of 4,4-dimethyloxazoline (DMOX) derivatives confirmed that the major 16:1 isomer was 16:1 n-7 (Δ9). Together, these results establish *P. moriformis* as a scalable fermentation platform for producing POA-rich oil and highlight its potential as an efficient alternative source of POA, providing a foundation for further strain and process optimization toward commercial production.

Keywords: palmitoleic acid; *Prototheca moriformis*; heterotrophic microalga; genetic engineering; Δ9 desaturase; microbial oil; fermentation

1. Introduction

Palmitoleic acid (POA; 16:1 n-7 or *cis*-9 16:1) is a monounsaturated fatty acid (FA) produced endogenously in mammals through stearoyl-CoA desaturase-1 (SCD1)-mediated desaturation of palmitic acid and has been proposed to function as a "lipokine" involved in crosstalk between adipose tissue metabolism, insulin sensitivity, and hepatic lipid handling [1,2]. The evidence supporting these roles, however, differs substantially by study type. In animal and cell-based experimental models, exogenous POA has been reported to improve indices of insulin resistance, reduce hepatic lipid accumulation, and modulate inflammatory signaling, including AMP-activated protein kinase (AMPK)-dependent effects on macrophage polarization [1,3–5]. In humans, much of the available evidence is observational: circulating or dietary biomarkers of POA, particularly *trans*-POA associated with dairy fat, have been linked with more favorable metabolic profiles and a lower incidence of some metabolic syndrome-related risk factors, including differences in lipid fractions and glycemic markers [2,6–8]. Human intervention data are more limited and generally

Academic Editor: Tiago Lima de Albuquerque

Received: 12 January 2026
Revised: 10 March 2026
Accepted: 14 March 2026
Published: 18 March 2026

suggest effects on selected lipid endpoints, with some studies reporting reductions in LDL-cholesterol and related lipid ratios, little change in triglycerides, and neutral to modestly favorable effects on HDL cholesterol [9–12]. Overall, dose–response relationships and the clinical efficacy of POA in humans are not yet firmly established.

In skin biology, 16:1 monoenes such as sapienic acid (16:1 n-10) and POA are localized in different epidermal and sebaceous lipid compartments. POA has been detected in living epidermis and stratum corneum, whereas sapienic acid predominates in human sebum and the surface lipid film [13–15]. These distribution patterns are consistent with possible roles in membrane and barrier lipid organization, and early experimental studies suggest that 16:1 species can inhibit Gram-positive bacteria [16,17]. Additional in vitro studies indicate that POA and related 16:1 fatty acid species can exert selective antimicrobial activity against skin-associated organisms such as *Staphylococcus aureus* and *Cutibacterium acnes* under experimental conditions [16,18]. Human clinical evidence in this area remains limited. Randomized controlled trials of oils enriched in POA have reported improvements in skin hydration, barrier-related measures, elasticity, and wrinkle-associated parameters, while evidence related to photoaging and acne has emerged primarily from mixed formulations or multi-nutrient regimens in which the specific contribution of POA cannot be isolated [19–21]. Taken together, these findings support continued interest in POA as a biologically relevant lipid in metabolism and skin physiology, but the evidence base remains heterogeneous across in vitro systems, animal models, observational human studies, and a relatively small number of intervention trials. Further mechanistic studies, well-controlled clinical trials, and dose–response evaluations in humans are needed before clear conclusions can be drawn regarding clinical efficacy or optimal applications.

From a dietary perspective, the richest botanical sources of POA include sea buckthorn pulp oil, followed by macadamia oil, and to a lesser extent, avocado oil, all of which provide meaningful levels compared with most conventional vegetable oils. Additionally, marine foods provide more modest dietary contributions of POA [22–28].

The production of POA by fermentation via microbial strains has been investigated in several engineered strains, including *Yarrowia lipolytica* [29], *Saccharomyces cerevisiae* [30,31], *Scheffersomyces segobiensis* [32], *Escherichia coli* [33], and *Komagataella phaffii* (formerly *Pichia pastoris*) [34]. Broader screening and condition-optimization studies in yeasts, including *Candida krusei* and *Kluyveromyces polysporus* [35], have also been reported. Outcomes range from high POA enrichment in yeast biomass to the development of high-titer secretion platforms for POA-rich free FA. In engineered *Y. lipolytica*, POA reached 50.6% of total FA, with a POA titer of 25.6 g/L in the bioreactor [29]. In *S. cerevisiae*, a 5 L fermenter run resulted in 57.5% POA with a titer of 6.6 g/L, building on earlier cultivation-based optimization that reported ~55% POA in a shake-flask run [31]. In *S. segobiensis*, a POA-targeted lipid production strategy delivered 7.3 g/L POA in a bioreactor [32]. In bacterial systems, engineered *E. coli* strains achieved a total free fatty acid (FFA) titer of 33.6 g/L and a POA content of 30.3%, corresponding to a final POA titer of approximately 10 g/L in batch fermentation [33]. In a secretion-oriented yeast platform, engineered *K. phaffii* increased POA from 5.5% to 22.0% and produced 0.37 g/L extracellular POA, yielding a total POA production of 0.61 g/L [34]. Finally, a screening and optimization program across diverse yeast species identified high-performance POA producers under defined nutrient ratios. Notably, *C. krusei* produced POA at titers of up to 430 mg/g dry weight under a carbon-to-nitrogen (C/N) ratio of 30 and a carbon-to-phosphorus (C/P) ratio of 6, while *K. polysporus* achieved a POA concentration of 74.5% under selected conditions [35].

In the present study, we report the first genetically engineered high-POA-producing strain of the heterotrophic microalga *Prototheca moriformis*, a chassis previously demonstrated to achieve high-cell-density oil production at scale [36].

2. Materials and Methods

2.1. Strain and Biolistic Transformation

Wild-type *P. moriformis* strain isolate UTEX 1533 was genetically engineered to enhance POA production obtained by fermentation. For transformation, base strain cells were cultivated in vegetative growth medium for 16–24 h with an initial cell density of 1×10^5 cells/mL, pelleted by centrifugation, then resuspended in phosphate-free culture medium to 1.25×10^8 cells/mL. Approximately 5×10^7 cells were plated onto selective solid medium containing phosphite as the sole phosphorus source. Plates were allowed to dry under sterile conditions in a biosafety cabinet prior to particle bombardment using gold nanoparticles. Primary transformants were selected by their ability to grow on phosphite-containing medium. For primary phenotypic screening, these transformants were cultivated in lipid production medium in a 96-well plate format (28 °C, 72 h, pH 7.0; with shaking at 900 rpm). FA profiles were determined by harvesting and lyophilizing biomass from each well, followed by the generation of fatty acid methyl esters (FAMEs) by direct transesterification and their subsequent analysis by gas chromatography–flame ionization detection (GC-FID).

2.2. Vector Construction

A gene fragment encoding the 394-amino-acid *Macadamia integrifolia* Δ9-desaturase (*MiSAD1618*) flanked by *Avr*II and *Pac*I restriction sites was synthesized by GenScript (Piscataway, NJ, USA). This fragment was inserted into an expression cassette designed for site-directed genomic integration at the Thi4a locus, utilizing 0.7–0.8 kb homology arms to enable targeted recombination. The cassette comprised the *MiSAD1618* coding sequence under the control of pNH4T (ammonia transporter promoter), an ammonium-responsive, pH-regulated promoter native to *P. moriformis*, as previously described [37]. The pNH4T promoter is activated under neutral pH conditions during nitrogen-limited lipid accumulation, enabling inducible expression without the addition of an external chemical inducer. Accordingly, both nitrogen limitation and pH shift to 7.0 induced promoter activation during the lipid production phase in tube-scale, flask-scale, and bioreactor cultivations [37]. The *P. moriformis* phosphoglycerate dehydratase (PGH) was used as the 3′ untranslated region (UTR), coupled with a phosphite dehydrogenase (PtxD from *Pseudomonas stutzeri*, WP_003118429.1) gene expression cassette as a selectable marker. The *MiSAD1618* expression cassette was designed to allow tandem integration at the target locus, with repeated regulatory elements flanking the coding region to facilitate gene amplification during particle bombardment-mediated transformation (Figure 1A,B). The linearized construct was transformed into wild-type *P. moriformis* cells, and individual colonies were subsequently screened for POA production. Correct genomic integration of the expression cassette was confirmed by PCR-based genotyping. Target integration at the intended locus was verified by PCR using primer pairs spanning the 5′ and 3′ junctions, with one primer annealing to the host genome outside the homology arm and the other annealing within the integrated cassette (Table S1).

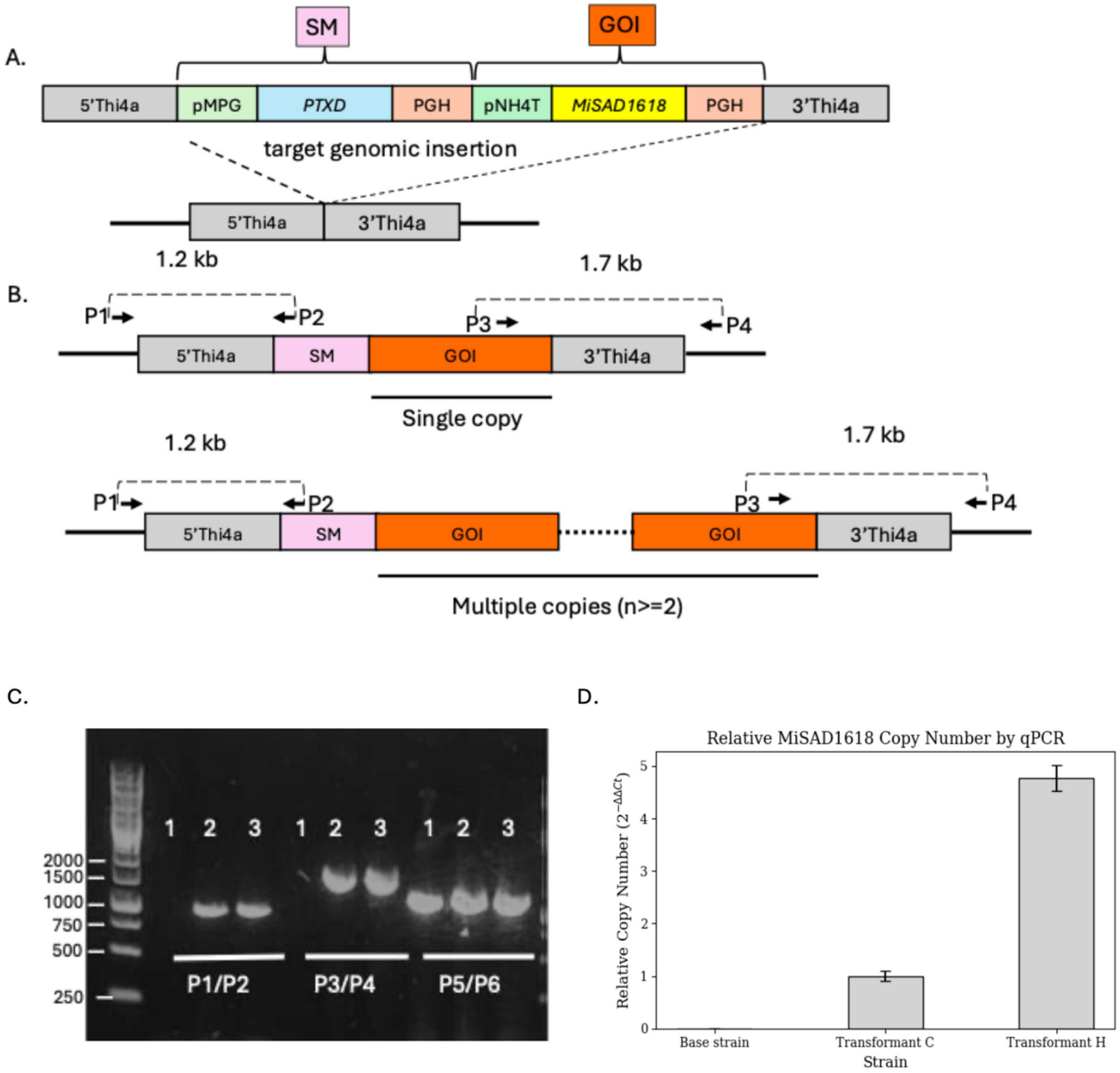

Figure 1. Confirmation of target integration and copy number of the *MiSAD1618* expression cassette. (**A**) Schematic of the expression construct used for target genomic integration at the *Thi4a* locus. (**B**) Schematic illustration of single-copy and multiple-copy cassette integration scenarios at the *Thi4a* locus. (**C**) PCR-based genotyping of transformants using primer spanning the 5′ and 3′ genome-cassette junctions (P1/P2 and P3/P4, respectively). Primer pair P5/P6 amplifying an endogenous locus was included as a genomic DNA quality control. Lane labels indicate base strain (1), Transformant C (2) and Transformant H (3). (**D**) TaqMan qPCR-based estimation of relative *MiSAD1618* copy number normalized to the endogenous reference gene *G2201*.

Quantitative PCR (qPCR) was performed using Custom TaqMan gene expression assay with FAM-labeled probes (Thermo Fisher Scientific, Waltham, MA, USA, Cat No. 4331348). Genomic DNA was isolated from transformants and the parental strain and treated with RNase. Custom primer–probe sets bound the introduced Δ9-desaturase gene *MiSAD1618* and the endogenous reference gene *G2201*. Reactions were prepared using TaqMan universal Master Mix and run on a real-time PCR system according to the manufacturer's recommended cycling conditions. Relative cassette abundance was calculated using

the comparative Ct (ΔΔCt) method by normalizing cassette Ct values to the endogenous reference locus and calibrating to the parental strain. Whole-genome sequencing was performed to evaluate the genomic integration and estimate the relative copy number of the *MiSAD1618* expression cassette in selected transformants (Angstrom Innovation, Berkeley, CA, USA). Sequencing reads were aligned to reference sequences corresponding to *MiSAD1618* and endogenous reference genes using a long-read alignment pipeline. Gene-level coverage statistics, including percentage coverage and mean sequencing depth across the full coding region, were calculated for each locus. *P. moriformis* is a diploid organism; therefore, sequencing depth for endogenous reference genes was normalized on a per-copy basis by dividing total depth by two, corresponding to the average depth per allelic copy. Relative *MiSAD1618* copy number was estimated by comparing its normalized mean depth to that of the endogenous reference genes within each strain.

2.3. Culture Media Composition and Conditions

Vegetative growth medium contained NaH_2PO_4 (13.6 mM), K_2HPO_4 (11.4 mM), citric acid monohydrate (5 mM), $MgSO_4{\cdot}7H_2O$ (5 mM), $CaCl_2{\cdot}2H_2O$ (0.155 mM), dextrose (40 g/L), $(NH4)_2SO_4$ (7.5 mM), and Sigma antifoam 204 (0.022%). The vegetative medium was supplemented with thiamine HCl (2.96×10^{-6} M), D-pantothenic acid (224 nM), biotin (6.53 nM), cyanocobalamin (83 pM), riboflavin (133 nM), and pyridoxine HCl (127 nM), and further contained micronutrients including H_3BO_3 (296 mM), $ZnSO_4{\cdot}7H_2O$ (12.2 µM), $MnSO4{\cdot}H_2O$ (14,6 µM), $NaMoO_4{\cdot}2H_2O$ (397 nM), $Ni(NO_3)_2{\cdot}6H_2O$ (275 nM), citric acid monohydrate (195 µM), $CuSO_4{\cdot}5H_2O$ (396 nM), and $FeSO_4{\cdot}7H_2O$ (5.4 µM). Vitamin and micronutrient components were maintained at the same concentrations in lipid production medium, while macronutrients were adjusted relative to vegetative medium: the lipid production medium was supplemented with 100 mM PIPES buffer (pH 7.0), the dextrose concentration was increased to 50 g/L, and $(NH4)_2SO_4$ decreased to 1.5 mM. The vegetative medium was adjusted to pH 6.0, and the lipid medium was buffered by PIPES and adjusted to pH 7.0 with KOH to induce the pNH4T promoter driving *MiSAD1618* expression. Cultures grown in tubes (10 mL) were incubated at 28 °C with shaking at 200 rpm for 72 h, while cultures in deep well 96-well block-format (500 µL) were incubated at 28 °C with shaking at 900 rpm in a Multitron incubator (Infors HT, Basel, Switzerland).

2.4. Flask Run Conditions in 1 L Bioreactor

Flask fermentation was conducted using the lipid production medium described in Section 2.3 under conditions similar to tube culture experiments. Initial cultures were inoculated into a working volume of 600 mL with 50 g/L batch glucose, agitated at 900 rpm, buffered with 100 mM PIPES (pH 7.0), and supplied with overlay aeration at 2 vvm. Fermentation was carried out at 28 °C for a duration of 96 h.

2.5. Fermentation at 1 L Bioreactor Scale

Transformant H was cultivated in 1 L glass bioreactors (250 mL working volume) in a phosphate-buffered POA basal medium containing (per liter): NaH_2PO_4 (33.1 mM), KH_2PO_4 (23.1 mM), $MgSO_4{\cdot}7H_2O$ (56.2 mM), $CaCl_2$ (0.544 mM), $(NH_4)_2SO_4$ (25.0 mM; equivalent to 50 mM NH_4^+), and Antifoam 204 (0.1%, *v*/*v*). The same trace metal and vitamin supplements used for the tube- and block-format cultures were also included in the batched fermentation medium at identical final (1×) concentrations. Basal medium was autoclaved (121 °C, 30 min), after which glucose and sterile supplements were added post-sterilization. Glucose was batched at 40 g/L and maintained in excess using a dissolved-oxygen-stat (DO-stat) feeding strategy, with bolus additions triggered by increases in dissolved oxygen (DO) indicative of carbon exhaustion. Bioreactors were inoculated at 10% (*v*/*v*) using a shake-flask seed culture (OD_{750} of approximately 5) and operated at

28 °C and pH 7.0. Two nitrogen regimes were evaluated: a high-nitrogen, high-cell-density condition (HCD) and a low-nitrogen, low-cell-density condition (LCD). In the HCD condition, nitrogen was supplied as 50 mM NH_4^+ equivalents in the batch medium (as $(NH_4)_2SO_4$), with additional nitrogen delivered during cultivation as NH_4OH, which also served as the primary base for pH control (total nitrogen of 250 mM as NH_4^+ equivalents). In the LCD condition, nitrogen was supplied solely as batched $(NH_4)_2SO_4$ (50 mM NH_4^+ equivalents) with no NH_4OH feed. DO setpoints were maintained at 50% (HCD) or 80% (LCD).

2.6. Fatty Acid (FA) Analysis by Gas Chromatography (GC-FID)

FAs were quantified as FAMEs following direct transesterification with a sulfuric acid–methanol solution, as previously described [36]. Samples were analyzed using an Agilent 8890 gas chromatograph equipped with a split/splitless inlet and a flame ionization detector (Agilent Technologies, Palo Alto, CA, USA). Chromatographic separation was performed on an Agilent DB-WAX column (30 m × 0.32 mm × 0.25 um dimensions). A FAME standard mixture purchased from Nu-Chek Prep (Nu-Chek Prep Inc., Elysian, MN, USA) was injected to establish retention times. Response factor corrections were determined empirically previously using standard mixtures from Nu-Chek Prep. Methyl nonadecanoate (19:0) was used as an internal standard for quantitation of individual FAMEs. The coefficient of variation (CV) of the GC-FID method was less than 0.5% for major fatty acids, whereas minor components present at low abundance exhibited slightly higher variability.

2.7. Structural Analysis via Tandem Gas Chromatography–Mass Spectrometry (GC-MS)

4,4-Dimethyloxazoline (DMOX) derivatives of FA were prepared using a modified published procedure [38] by heating the oil sample (10 mg) directly with 2-amino-2-methyl-1-propanol (500 µL) under a nitrogen atmosphere at 180 °C overnight. The DMOX derivatives were analyzed via GC-MS, with conditions previously described [38].

3. Results

3.1. Engineering and Primary Screening of a High-POA Strain

The *P. moriformis* base strain was engineered to increase POA by expressing the *Macadamia integrifolia* Δ9 desaturase (*MiSAD1618*) under the control of the pNH4T promoter. Transformants were selected using the phosphite utilization marker (PsPtxD), and primary transformants were subsequently evaluated for FA composition. Eight selected transformants, along with the parental base strain, were analyzed for their major FA profiles (Table 1). POA content in the transformants ranged from 16.2% to 54.2% of total FA, while the base strain produced less than 1% POA under the same screening conditions. The variation in POA content is consistent with the cassette design, which allows tandem integration and is expected to generate differences in *MiSAD1618* copy number among transformants. The top-performing isolate, designated Transformant H, accumulated 54.2% POA, accompanied by a corresponding reduction in oleic acid (18:1 n-9; 28.3% vs. 58.5%) and linoleic acid (18:2 n-6; 3.7% vs. 8.3%), indicating successful diversion of palmitic acid (16:0) toward POA synthesis and an overall shift in the lipid pool from C18 to C16 monounsaturated species. Transformant C with 16.2% POA and Transformant H with 54.2% POA were selected for genotyping to confirm the genomic integration of *MiSAD1618*.

Table 1. Major fatty acid profile of the control and primary transformants of the base strain (N = 1 for each clone).

Transformant ID	16:0	16:1 n-7	18:1 n-9	18:2 n-6
A	16.6	38.6	36.1	4.3
B	17.2	33.3	38.2	5.9
C	25.2	16.2	44.8	7.5
D	22.5	27.2	39.9	6.9
E	23.2	25.0	40.3	7.0
F	18.1	31.6	37.0	6.9
G	14.5	43.2	31.8	5.4
H	9.8	54.2	28.3	3.7
Base strain	26.1	0.8	58.5	8.3

3.2. Confirmation of Cassette Integration

Correct genomic integration of the expression cassette was confirmed using a combination of PCR-based genotyping, whole-genome sequencing, and quantitative PCR. The expression construct consists of a selection marker (SM) and the gene of interest (GOI: *MiSAD1618*) driven by their respective promoters and terminators, flanked by 5′ and 3′ homology arms derived from the *Thi4a* locus to enable targeted genomic integration (Figure 1A). Genomic integration at the expected locus was assessed via PCR-based genotyping using primer pairs spanning the 5′ and 3′ junctions of the integration site. As shown in Figure 1B, primer pairs P1/P2 and P3/P4 (Table S1) were used to amplify the 5′ and 3′ genome–cassette junctions, respectively. PCR amplification yielded products of expected size (1.2 kb for the 5′ junction and 1.7kb for the 3′ junction) in the Transformants C and H, whereas no corresponding products were detected in the base strain, supporting correct target integration at the *Thi4a* locus. In addition, primer pair P5/P6 amplified an endogenous control locus (*G2060*), validating genomic quality and PCR amplifiability across all three samples (Figure 1C).

Transformant C and H exhibited substantially different levels of palmitoleic acid (POA) accumulation (16.2% and 54.2%, respectively), suggesting differences in the genomic copy number of the integrated expression cassette. As illustrated in Figure 1B, these two outcomes are represented schematically as single-copy and multiple-copy cassette integration at the target locus, respectively. The GOI is flanked by two repeated sequences (Figure 1A). This 3kb region is designed for gene amplification during transformation. The above P3/P4 primer pair validated genomic integration at the target locus, and we employed quantitative PCR (qPCR) and whole-genome sequencing to detect GOI copy number. Taqman probe-based qPCR analysis was performed to estimate the relative abundance of the heterologous Δ9-desaturase gene (*MiSAD1618*) compared to the endogenous reference gene (*G2201*) (primer–probe sets are shown in Table S1). The relative copy number was calculated using the ΔΔCt method, with Transformant C defined as the calibrator and set to 1x. This analysis showed that Transformant H contained an approximately five-fold higher relative abundance of *MiSAD1618* compared with Transformant C, whereas the base strain displayed only a background-level signal (Figure 1D).

Whole-genome sequencing (WGS) coverage analysis was performed to evaluate the genomic integration and relative copy number of the heterologous Δ9-desaturase gene (*MiSAD1618*). Complete coverage of the *MiSAD1618* coding sequence was observed in both Transformant H and Transformant C, with 100% of bases covered, indicating intact integration of the expression cassette in both strains. However, the sequencing depth of *MiSAD1618* was substantially higher in Transformant H than in Transformant C, suggesting increased genomic copy number in Transformant H. To estimate relative copy number, *MiSAD1618* coverage was normalized to the average depth of two endogenous

reference genes, *G2201* and *G1295*. Using this combined reference, WGS depth analysis estimated *MiSAD1618* copy numbers of approximately 2.79 in Transformant H and 0.66 in Transformant C, corresponding to an approximately 4.2-fold higher genomic copy number of *MiSAD1618* in Transformant H compared with Transformant C. Independent qPCR and whole-genome sequencing analyses consistently indicated higher genomic copy number of *MiSAD1618* in Transformant H compared to Transformant C, with qPCR and WGS estimating approximately five-fold and fourfold difference, respectively.

3.3. Lipid Production in Tube and 600 mL Flask Culture

To quantify lipid accumulation in addition to fatty acid composition analysis, the top-performing engineered strain (Transformant H) and the parental control were cultivated in pH 7.0 lipid production medium in 10 mL tubes at 28 °C for 72 h. Under these conditions, the engineered strain retained a POA-enriched profile of 53.9%, with a dry cell weight (DCW) of 2.98 g/L, a lipid content of 50.0% (DCW-based), and a lipid titer of 1.49 g/L (Table 2). In contrast, the parental base strain produced 0.78% POA while maintaining a higher lipid titer under the same tube-based assay conditions. These results indicate that the genetic modification altered FA partitioning toward POA. To confirm POA enrichment beyond the initial small-scale screening, oil samples obtained from subsequent 600 mL shake-flask cultivation were analyzed via GC-FID (Figure 2). In this flask cultivation, the engineered strain contained 58.2% POA at 96 h, accompanied by the anticipated composition shifts, including reductions in oleic acid (18:1 n-9; 23.8% vs. 58.5% in the base strain) and palmitic acid (16:0; 7.9% vs. 26.1% in the base strain). This shift confirms that the POA-enrichment phenotype is stable and reproducible from tube to flask-scale cultivation.

Table 2. Tube assay lipid metrics and palmitoleic acid (16:1 n-7) concentration in the control and transformed strain H at 72 h (N = 4). Mean and standard deviation are shown.

Sample Name	Lipid Content (% DCW)	DCW (g/L)	Oil Titer (g/L)	16:1 n-7 (% of Total FA)
Transformant H	50.03 ± 1.29	2.98 ± 0.15	1.49 ± 0.05	53.9 ± 2.33
Control base strain	57.13 ± 1.07	8.71 ± 0.25	5.02 ± 0.20	0.78 ± 0.01

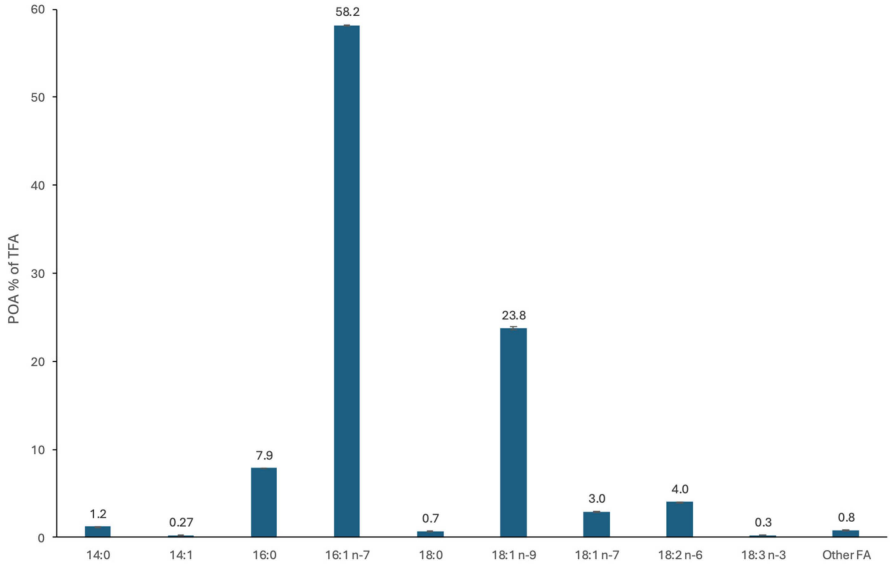

Figure 2. Fatty acid profile (expressed in % of total fatty acid) of microbial oil from the engineered high-POA *P. moriformis* strain Transformant H grown in 600 mL shake-flask cultures. The experiment was performed in technical triplicate.

3.4. Evaluation of POA Production in Bioreactor Cultivation

The POA-enriched strain (Transformant H) was further evaluated in 1 L bioreactors at 28 °C and pH 7.0 (63 mM monobasic phosphate buffer) under two nitrogen and dissolved oxygen (DO) regimes to assess their effects on lipid accumulation and POA enrichment (Table 3). Under the high-nitrogen condition (250 mM NH_4^+; 70% DO), lipid titer increased from 21 g/L at 51 h to 46 g/L at 77 h and reached 48 g/L at 96 h, while POA content remained high (46.67% at 51 h and 43.53% at 96 h). Under the low-nitrogen condition (50 mM NH_4^+; 80% DO), the lipid titer increased from 15.4 g/L at 51 h to 33.7 g/L at 94 h, with POA maintained at approximately 41–45% of total fatty acids across all time points.

Table 3. Lipid titer and palmitoleic acid (16:1 n-7) composition of the engineered *P. moriformis* strain (Transformant H) under different nitrogen and dissolved oxygen conditions in 1 L bioreactor cultivations. Values for lipid titer and POA (%) are reported as mean ± SD (N = 4) from two independent bioreactor runs with duplicate analytical measurements.

Condition	EFT (h)	NH_4^+ (mM)	DO (%)	Lipid Titer (g/L)	POA (% of TFA)
Low N/high DO	51	50	80	15.1 ± 0.2	45.0 ± 0.2
Low N/high DO	77	50	80	28.7 ± 1.7	41.7 ± 0.1
Low N/high DO	94	50	80	33.1 ± 0.5	41.1 ± 0.3
High N/moderate DO	51	250	70	20.9 ± 0.2	46.6 ± 0.1
High N/moderate DO	77	250	70	46.7 ± 1.2	43.4 ± 0.2
High N/moderate DO	96	250	70	47.8 ± 0.4	43.5 ± 0.1

These results demonstrate that high POA enrichment is maintained during process scale-up and that increased nitrogen availability supports substantially higher lipid titers. However, POA levels in the bioreactor were lower than those achieved in tube (53.9%) and shake-flask (58.2%) cultures. This moderate reduction may reflect differences in bioreactor operating conditions, including dissolved oxygen and mixing and nutrient supply dynamics, which may influence the activity of the heterologous Δ9-desaturase or alter fatty acid flux toward POA biosynthesis.

3.5. Structural Confirmation of the 16:1 (n-7) Isomer via GC-MS Analysis

To confirm the identity of the 16:1 isomers present in the oil produced by engineered *P. moriformis*, GC–MS analysis was performed to verify the double-bond position of the predominant 16:1 FAME peak, which had been tentatively assigned as 16:1 (n-7) based on comparison with authentic standards (double bond at the Δ9 position; see Figure 3). Oil recovered from the primary screening was converted to DMOX derivatives and analyzed via GC–MS to verify the identity of the 16:1 species enriched in the genetically engineered strain. The mass spectrum of the DMOX derivative of 16:1 (n-7) displayed several distinctive features, including a prominent molecular ion at a mass-to-charge ratio m/z 307 and a diagnostic 12 amu gap between m/z 196 and 208, consistent with a double bond between carbons 9 and 10 ([39]; Supplementary Figure S1). Together, these spectral characteristics confirmed that the enriched 16:1 isomer in the engineered strain was palmitoleic acid (POA; 16:1 n-7).

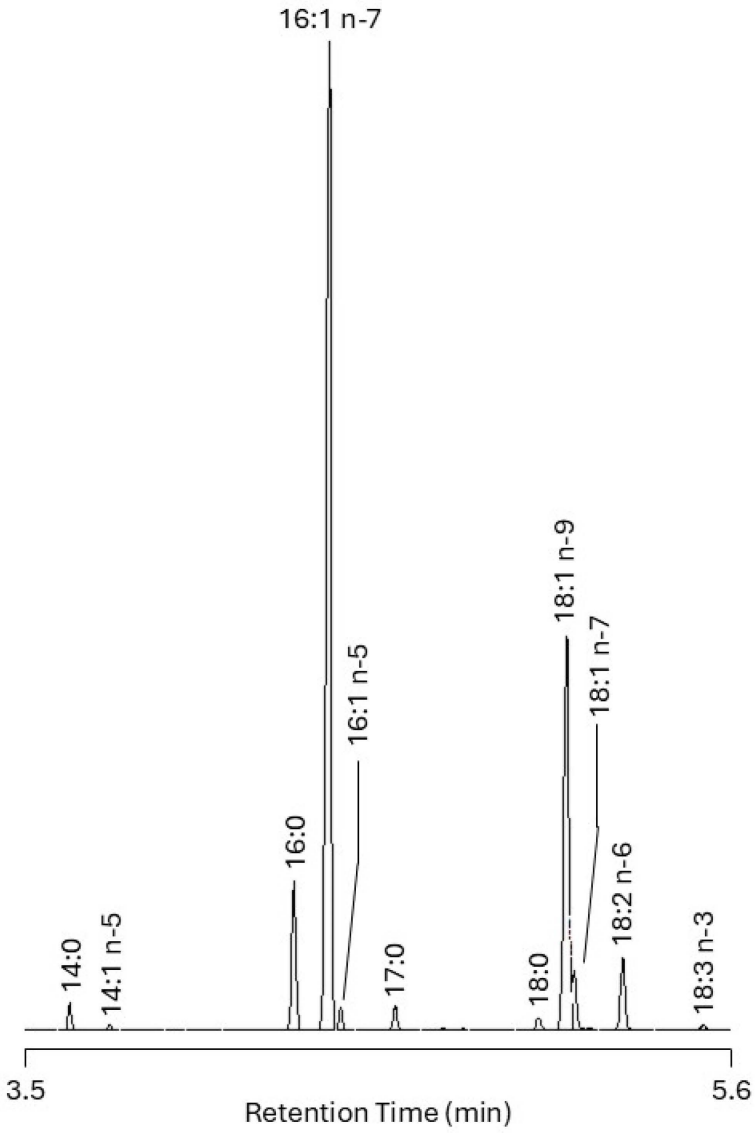

Figure 3. Chromatographic separation highlights the fatty acids in engineered *P. moriformis* oil. The dominant 16:1 peak corresponds to palmitoleic acid (16:1 n-7, Δ9). Peak identity was confirmed via GC–MS analysis of DMOX derivatives (Supplementary Figure S1).

4. Discussion

Introducing the *Macadamia integrifolia* Δ9-desaturase (*MiSAD1618*) into *P. moriformis* resulted in a substantial increase in palmitoleic acid (POA) production, indicating that enhanced C16 desaturation is an effective way to redirect lipid flux toward omega-7 fatty acids. The wide variation in POA levels across transformants suggests that differences in genomic integration and gene dosage have a major impact on strain performance. In the highest-producing strain, Transformant H, the increase in POA was accompanied by lower levels of C18 unsaturated fatty acids, consistent with palmitic acid being preferentially directed toward Δ9 desaturation rather than elongation to C18 fatty acids. Overall, these results support *P. moriformis* as a useful platform for POA production and provide a clear foundation for further genetic analysis of representative low- and high-producing strains.

Among the engineered strains, Transformants H and C represented the extremes of palmitoleic acid (POA) production, with high and low POA levels, respectively. This marked phenotypic difference suggested that variation in the genomic integration of the *MiSAD1618* expression cassette, such as differences in copy number, could underline the observed range in POA accumulation. To test this possibility, these two transformants

were selected for further molecular characterization, including copy-number analysis using both qPCR and whole-genome sequencing (WGS). Estimates of the *MiSAD1618* genomic copy number obtained by qPCR and WGS showed minor quantitative differences but were consistent in overall trend. qPCR indicated that *MiSAD1618* abundance in Transformant H was approximately five-fold higher than in Transformant C, whereas WGS coverage analysis suggested a slightly lower, approximately four-fold difference. Such variation is expected given the different principles underlying the two methods, with qPCR measuring amplification of a short target region, and WGS relying on sequencing depth across the full gene. Despite these differences, both approaches consistently indicate a substantially higher *MiSAD1618* copy number in Transformant H relative to Transformant C, supporting a link between increased gene dosage and enhanced POA production through increased Δ9-desaturase activity that promotes the conversion of palmitic acid (16:0) to POA (16:1 n-7).

Tube, flask, and bioreactor experiments demonstrate that the POA-enriched phenotype of Transformant H is maintained as cultivation progresses from low-cell-density screening to high-cell-density fermentation. POA levels exceeded 50% in tube and flask cultures and remained at relatively high levels (~41–47%) in 1 L bioreactors under both nitrogen regimes, indicating that *MiSAD1618* activity is preserved during scale-up. In the bioreactor, increased nitrogen availability supported substantially higher lipid titers, reaching nearly 50 g/L, while the POA fraction decreased moderately compared with small-scale cultures. The differences in POA composition observed between small-scale and high-cell-density bioreactors likely reflect several process-related factors that influence fatty acid metabolism. Tube and shake-flask cultures typically operate at relatively low biomass concentrations with passive aeration and minimal environmental gradients, conditions that may favor desaturase activity and the formation of unsaturated fatty acids.

Oxygen availability is one important difference distinguishing tube and shake-flask cultures from bioreactors. Δ9-desaturase enzymes catalyze the conversion of palmitic acid (16:0) to palmitoleic acid (16:1 n-7) through an oxygen-dependent reaction, making dissolved oxygen (DO) a key parameter affecting fatty acid desaturation. For example, in *S. segobiensis*, maintaining higher DO levels increases the proportion of 16:1 from 13.0% under uncontrolled DO conditions to 16.4% and 19.9% when DO was maintained above 20% and 40%, respectively, accompanied by a decrease in 18:1 levels. Similar effects of oxygen on fatty acid composition have also been reported in *Lipomyces starkeyi*, *Y. lipolytica*, and *Rhodotorula* species [40]. Although DO was controlled in the bioreactor, the high oxygen demand associated with high cell density may still lead to transient oxygen limitation, potentially reducing Δ9-desaturase activity and lowering the relative POA fraction. More broadly, high-cell-density physiology can impose additional metabolic constraints that are absent in small-scale cultures. Increasing biomass concentrations elevate cellular oxygen demand, alter intracellular redox balance, and increase flux through central carbon metabolism, which may further influence the availability of reducing equivalents and cofactors required for desaturation reactions and contribute to the observed shift in fatty acid composition [34,41]. Rapid TAG assembly during high-flux lipid accumulation may also reduce the time available for complete desaturation of fatty acid intermediates, allowing a greater proportion of palmitic acid (16:0) to be incorporated directly into lipid pools before conversion to POA. Furthermore, even when expressed heterologously, Δ9-desaturase activity can be affected by substrate availability, membrane composition, and cellular redox state, which may further contribute to the differences in POA fraction observed between small-scale cultures and bioreactor conditions.

The nitrogen regime may also contribute to the observed change in POA fraction during the scale-up. In the present study, higher nitrogen availability supported substantially higher lipid titers, approaching 50 g/L. However, nitrogen levels are known to influence

carbon flux distribution within lipid metabolic pathways in oleaginous microorganisms. For example, Kolouchová and colleagues [35] reported that increasing the C/N ratio from 3 to 30 significantly altered fatty acid composition in several yeast species, including changes in the proportion of palmitoleic acid (16:1), demonstrating that nutrient conditions can modulate fatty acid desaturation and elongation pathways. Under high-nitrogen conditions, rapid biomass formation and lipid assembly may reduce the extent of fatty acid modification, allowing palmitic acid (16:0) to be incorporated into lipids or redirected toward elongation before complete conversion to POA. This may partially explain the lower relative POA fraction observed during high-cell-density fermentation despite increased overall lipid production [35].

Taken together, the reduced POA fraction observed at the bioreactor scale likely reflects a process-dependent trade-off between lipid titer and fatty acid composition rather than a limitation of the engineered strain. Importantly, the POA-enriched phenotype remained robust under all fermentation conditions tested, indicating that the underlying metabolic engineering strategy remains effective during scale-up. As summarized in Table 4, recent efforts to develop fermentation-derived sources of POA have focused on simultaneously increasing the fraction of POA within cellular lipids and improving overall lipid or free fatty acid titers. Across microbial hosts, the most effective strategies combine expansion of the intracellular palmitic acid (16:0) pool; introduction or upregulation of C16-specific Δ9-desaturases; attenuation of competing elongation pathways leading to C18+ fatty acids; and optimization of lipid assembly, secretion, and stability through enhanced triacylglycerol (TAG) or free fatty acid formation. These approaches have enabled substantial POA production in several engineered systems, including *Y. lipolytica*, *S. cerevisiae*, *S. segobiensis*, *K. phaffii*, and *E. coli*, with reported POA titers ranging from sub-gram levels to more than 25 g/L depending on the host and fermentation strategy (Table 4).

Among these systems, engineered *Y. lipolytica* achieved one of the highest reported POA titers (25.6 g/L) with a productivity of approximately 0.13 g/L/h under optimized fermentation conditions, including a temperature shift from 30 °C to 20 °C during production, and the POA fraction reached around 50% of total fatty acids [29]. In contrast, engineered *S. cerevisiae* strains have demonstrated higher POA enrichment, reaching up to 57% of total fatty acids under optimized temperature-controlled fermentation conditions, but with lower titers and productivities of approximately 0.05 g/L/h [30,31]. Other yeast systems, including *S. segobiensis* and *K. phaffii*, have achieved moderate POA titers and productivities, typically around 7 g/L and 0.04 g/L/h or lower depending on the system [32,34]. Bacterial platforms such as engineered *E. coli* can produce relatively high levels of free fatty acids, with estimated POA titers exceeding 10 g/L and estimated POA productivity approaching 0.7 g/L/h, although these systems generally produce mixed fatty acid pools rather than POA-rich lipids [33]. Process parameters also play an important role in controlling the fatty acid composition. Temperature, for example, has been reported to influence fatty acid desaturation in many microorganisms through regulation of membrane fluidity, with lower cultivation temperatures often promoting the formation of monounsaturated fatty acids such as POA. Consistent with this mechanism, several engineered yeast platforms have incorporated reduced or staged cultivation temperatures to enhance POA enrichment during fermentation, as reflected in the temperature-shift strategies used in *Y. lipolytica* and *S. cerevisiae* described above [29–31].

Table 4. Overview of engineered and selected microbial platforms for palmitoleic acid (POA; 16:1 n-7) production. The table summarizes representative host organisms, the key genetic or process strategies employed, the maximum POA content (expressed as percentage of total fatty acids, total lipids, or secreted free fatty acids as indicated), and the corresponding POA titers achieved in laboratory or pilot-scale fermentations. POA titer values are reported as directly measured or, where indicated, estimated (est.) or calculated (calc.) from published lipid and composition data; NR, not reported.

Microorganism	Ref.	Strategy/Key Modifications	POA Content (Basis)	POA Titer (g/L) [Fermentation Time]	POA Productivity (g/L/h)
Yarrowia lipolytica	[29]	Two-layer strategy: C16-specific Δ9 desaturase + dynamic elongation control; lipid-accumulation modules; reduced lipid degradation; (30 °C→20 °C)	51% of total FAs (max); 46.7% TFA in 5 L fermentation	25.6 [192 h]	0.13
Saccharomyces cerevisiae	[30]	FA-profile engineering (elongation/desaturation control) + process optimization; two-stage temperature shift (30 °C→20 °C)	57% of total FAs	6.56 [144 h]	0.05
Saccharomyces cerevisiae	[31]	DGA1ΔN expression in Δdga1 background; methionine supplementation; low temperature	Up to 55% of total FAs	NR	NR
Saccharomyces cerevisiae	[42]	Reprogramming metabolism from ethanol fermentation to lipogenesis; improved secretion of FFAs	NR	NR	NR
Scheffersomyces segobiensis	[32]	Transcriptomics-guided lipid gene overexpression; Xpk/Pta acetyl-CoA module; O–S dynamic regulation	25% of lipid	7.3 [186 h]	0.04
Komagataella phaffii (*Pichia pastoris*)	[34]	Metabolic engineering for POA enrichment, reduced FFA recycling and enhanced export	~19% of secreted FFAs (best strain)	0.37 (secreted); 0.61 (total) [148 h]	0.004
Komagataella phaffii (Pichia pastoris)	[43]	Methanol-based fatty acid derivatives production platform; enhanced acetyl-/malonyl-CoA and redox supply	NR (54% unsaturated FAs total)	NR	NR
Kluyveromyces polysporus,	[35]	Strain screening and nutrient ratio optimization (C/N and C/P)	34–74% of total FAs	NR	NR
Escherichia coli	[33]	Combinatorial metabolic engineering for high FFA secretion	30% C16:1 in FFAs	10.2 (calc.) [57 h]	0.18
Escherichia coli	[44]	Chain-length control + hydroxylation (P450); FA synthesis rewiring for ω-hydroxy FAs	Not POA (ω-hydroxy FA product)	NR	NR
Prototheca moriformis	This study	Expression of *MiSAD1618* (*Macadamia integrifolia* Δ9 desaturase gene) in *P. moriformis*; strain screening and bioreactor validation	54% of total FAs (screening); 58% in shake-flask and 43% in 1 L bioreactor	20.8 (est., 1 L) [96 h]	0.22

In this study, we engineered the non-photosynthetic microalga *P. moriformis* to produce a POA-rich oil profile through expression of a heterologous macadamia Δ9-desaturase (*MiSAD1618*). The engineered strain achieved POA contents exceeding 50% of total fatty acids during small-scale screening and maintained high POA enrichment across subsequent cultivation formats. When the top-performing transformant was evaluated under high-cell-density 1 L bioreactor cultivation, a lipid titer of 48.0 g/L was achieved at 96 h

with POA comprising 43.5% of total fatty acids, corresponding to an estimated POA titer of approximately 20.8 g/L and an average productivity of approximately 0.22 g/L/h. Within the landscape of previously reported microbial platforms for POA production (Table 4), this performance is competitive in terms of POA enrichment, titer, and productivity. Importantly, prior work has demonstrated that *P. moriformis* can be translated to industrially relevant scales, including multi-m^3 fermentors, while sustaining very high biomass and lipid accumulation, reaching approximately 220 g dry cell weight per kg of fermentation broth and oil titers on the order of 150 g/L [36]. Together, these characteristics highlight *P. moriformis* as a promising and scalable eukaryotic chassis for producing POA-rich microbial oils. Further strain and process optimization, including improved oxygen transfer, refined feeding strategies, temperature control, and tuning of desaturase expression, may provide additional opportunities to further enhance both lipid titer and POA fraction. While the exact POA percentages observed in small-scale screening may not be fully reproduced under industrial high-cell-density conditions, targeted optimization of fermentation parameters and strain performance is expected to substantially improve POA enrichment while maintaining industrially relevant lipid titers.

5. Conclusions

In this study, we demonstrate that the heterotrophic microalga *P. moriformis* can be genetically engineered into an effective platform to produce POA-enriched oil through expression of a heterologous Δ9 desaturase (*MiSAD1618*). The engineered strains substantially increase POA content relative to the parental strain, confirming that this microalgal host effectively supports the targeted metabolic modification. Structural analysis by GC–MS of DMOX derivatives verified that the predominant 16:1 isomer produced was POA (16:1 n-7; Δ9), supporting the selectivity of the desaturase and the precision of the engineering strategy. Importantly, high POA enrichment was maintained during high-cell-density fermentation while achieving lipid titers relevant for industrial processes. Collectively, these results highlight its potential as a promising eukaryotic chassis for fermentation-based production of POA-enriched oils. Further improvements in strain engineering and fermentation process optimization will likely enhance both the POA fraction and overall productivity, supporting the development of green and sustainable microbial sources of omega-7 fatty acids for applications in nutrition, dietary supplements, cosmetics, and personal care applications.

Supplementary Materials: The following supporting information can be downloaded at: https://www.mdpi.com/article/10.3390/fermentation12030160/s1, The DMOX mass spectra of 16:1 n-7 (POA) identified in the oil produced from the engineered strain can be found as Supplementary Figure S1. Figure S1. Identification of double-bond position in monoenoic fatty acids by GC–MS of 4,4-dimethyloxazoline (DMOX) derivatives. (Mass spectrum of the DMOX derivative of 9-16:1 (16:1 n-7; POA). Table S1. Primers used in this study. Table S2. WGS coverage statistics used for copy number estimation.

Author Contributions: X.Z., L.P. and T.G. developed the algae strain. D.A., B.D. and L.E. performed the fermentation trials. C.P. and G.E. performed the extraction and refining of the algae oil samples. M.C. (Mona Correa). V.B. and M.C. (Marvin Cornejo) conducted all the analytical method development, quantification of fatty acids and structural analysis via GC-MS. F.D., M.O., X.Z., L.P., W.R., J.M.W. and J.C.L. wrote the manuscript draft. All authors have read and agreed to the published version of the manuscript.

Funding: This research was partially funded by Société des Produits Nestlé SA and Checkerspot.

Institutional Review Board Statement: Not applicable.

Informed Consent Statement: Not applicable.

Data Availability Statement: The original contributions presented in this study are included in the article/Supplementary Material. Further inquiries can be directed to the corresponding author.

Conflicts of Interest: All authors were employed by the company Checkerspot and declare no conflicts of interest. The authors declare that this study received funding from Société des Produits Nestlé SA. The funder was not involved in the study design, collection, analysis, interpretation of data, the writing of this article or the decision to submit it for publication.

Abbreviations

The following abbreviations are used in this manuscript:

AMPK	AMP-activated protein kinase
C/N	Carbon-to-nitrogen ratio
C/P	Carbon-to-phosphorus ratio
CV %	Coefficient of variation
DCW	Dry cell weight
DMOX	4,4-Dimethyloxazoline
DO	Dissolved oxygen
DO-stat	Dissolved-oxygen-stat
EFT	Elapsed fermentation time
FA	Fatty acid(s)
FAME	Fatty acid methyl ester
FFA	Free fatty acid
TFA	Total fatty acid
GC-FID	Gas chromatography–flame ionization detection
GC-MS	Gas chromatography–mass spectrometry
HCD	High-cell-density condition
HDL	High-density lipoprotein
HEPES	4-(2-hydroxyethyl)-1-piperazineethanesulfonic acid
LCD	Low-cell-density condition
LDL	Low-density lipoprotein
m/z	Mass-to-charge ratio
OD_{750}	Optical density at 750 nm
O–S	Oxygen–substrate (dynamic regulation strategy)
POA	Palmitoleic acid
PTXD	Phosphite dehydrogenase (selectable marker gene)
rpm	Revolutions per minute
SCD1	Stearoyl-CoA desaturase-1
TAG	Triacylglycerol
UTR	Untranslated region
v/*v*	Volume/volume
Xpk/Pta	Phosphoketolase/phosphotransacetylase

References

1. Cao, H.; Gerhold, K.; Mayers, J.R.; Wiest, M.M.; Watkins, S.M.; Hotamisligil, G.S. Identification of a lipokine, a lipid hormone linking adipose tissue to systemic metabolism. *Cell* **2008**, *134*, 933–944. [CrossRef]
2. Frigolet, M.E.; Gutiérrez-Aguilar, R. The role of the novel lipokine palmitoleic acid in health and disease. *Adv. Nutr.* **2017**, *8*, 173S–181S. [CrossRef] [PubMed]
3. Yang, Z.-H.; Miyahara, H.; Hatanaka, A. Chronic administration of palmitoleic acid reduces insulin resistance and hepatic lipid accumulation in KK-Ay mice with genetic type 2 diabetes. *Lipids Health Dis.* **2011**, *10*, 120. [CrossRef]
4. Souza, C.O.; Teixeira, A.A.S.; Lima, E.A.; Batatinha, H.A.P.; Rosa Neto, J.C. Palmitoleic acid (n-7) attenuates immunometabolic disturbances caused by a high-fat diet independently of PPARα. *Mediat. Inflamm.* **2014**, *2014*, 582197. [CrossRef]

5. Chan, K.L.; Pillon, N.J.; Sivaloganathan, D.M.; Costford, S.R.; Liu, Z.; Théret, M.; Chazaud, B.; Klip, A. Palmitoleate reverses high fat-induced proinflammatory macrophage polarization via AMP-activated protein kinase (AMPK). *J. Biol. Chem.* **2015**, *290*, 16979–16988. [CrossRef]
6. Mozaffarian, D.; Cao, H.; King, I.B.; Lemaitre, R.N.; Song, X.; Siscovick, D.S.; Hotamisligil, G.S. Trans-palmitoleic acid, metabolic risk factors, and new-onset diabetes in U.S. adults: A cohort study. *Ann. Intern. Med.* **2010**, *153*, 790–799. [CrossRef]
7. Mozaffarian, D.; de Oliveira Otto, M.C.; Lemaitre, R.N.; Fretts, A.M.; Hotamisligil, G.; Tsai, M.Y.; Siscovick, D.S.; Nettleton, J.A. Trans-Palmitoleic acid, other dairy fat biomarkers, and incident diabetes: The Multi-Ethnic Study of Atherosclerosis (MESA). *Am. J. Clin. Nutr.* **2013**, *97*, 854–861. [CrossRef]
8. Santaren, I.D.; Watkins, S.M.; Liese, A.D.; Wagenknecht, L.E.; Rewers, M.J.; Haffner, S.M.; Hanley, A.J. Serum pentadecanoic acid (15:0), a short-term marker of dairy food intake, is inversely associated with incident type 2 diabetes and its underlying disorders. *Am. J. Clin. Nutr.* **2014**, *100*, 1532–1540. [CrossRef] [PubMed]
9. Curb, J.D.; Wergowske, G.; Dobbs, J.C.; Abbott, R.D.; Huang, B. Serum lipid effects of a high-monounsaturated fat diet based on macadamia nuts. *Arch. Intern. Med.* **2000**, *160*, 1154–1158. [CrossRef] [PubMed]
10. Garg, M.L.; Blake, R.J.; Wills, R.B.H. Macadamia nut consumption lowers plasma total and LDL cholesterol levels in hypercholesterolemic men. *J. Nutr.* **2003**, *133*, 1060–1063. [CrossRef]
11. Griel, A.E.; Cao, Y.; Bagshaw, D.D.; Cifelli, A.M.; Holub, B.; Kris-Etherton, P.M. A macadamia nut-rich diet reduces total and LDL-cholesterol in mildly hypercholesterolemic men and women. *J. Nutr.* **2008**, *138*, 761–767. [CrossRef]
12. Hiraoka-Yamamoto, J.; Ikeda, K.; Negishi, H.; Mori, M.; Hirose, A.; Sawada, S.; Onobayashi, Y.; Kitamori, K.; Kitano, S.; Tashiro, M.; et al. Serum lipid effects of a monounsaturated (palmitoleic) fatty acid-rich diet based on macadamia nuts in healthy, young Japanese women. *Clin. Exp. Pharmacol. Physiol.* **2004**, *31*, S37–S38. [CrossRef]
13. Ansari, M.N.A.; Nicolaides, N.; Fu, H.C. Fatty acid composition of the living layer and stratum corneum lipids of human sole skin epidermis. *Lipids* **1970**, *5*, 838–845. [CrossRef]
14. Nicolaides, N. Skin lipids: Their biochemical uniqueness. *Science* **1974**, *186*, 19–26. [CrossRef]
15. Downing, D.T.; Strauss, J.S. Synthesis and composition of surface lipids of human skin. *J. Investig. Dermatol.* **1974**, *62*, 228–244. [CrossRef]
16. Wille, J.J.; Kydonieus, A. Palmitoleic acid isomer (C16:1Δ6) in human skin sebum is effective against gram-positive bacteria. *Skin Pharmacol. Appl. Skin Physiol.* **2003**, *16*, 176–187. [CrossRef]
17. Takigawa, H.; Nakagawa, H.; Kuzukawa, M.; Mori, H.; Imokawa, G. Deficient production of hexadecenoic acid in the skin is associated in part with the vulnerability of atopic dermatitis patients to colonization by Staphylococcus aureus. *Dermatology* **2005**, *211*, 240–248. [CrossRef] [PubMed]
18. Yamamoto, K.; Matsubara, Y.; Ando, Y.; Iwasaki, Y. Lubricant and bactericidal properties of calcium salts of fatty acids: Effect of degree of unsaturation. *J. Oleo Sci.* **2015**, *64*, 1095–1100. [CrossRef] [PubMed]
19. Koh, Y.G.; Park, J.S.; Kim, K.R.; Yoo, K.H.; Kim, Y.J.; Kim, B.J. Efficacy and safety of oral palmitoleic acid supplementation for skin barrier improvement: A 12-week, randomized, double-blinded, placebo-controlled study. *Heliyon* **2023**, *9*, e16711. [CrossRef] [PubMed]
20. Sung, H.K.; Kim, T.J.; Kim, H.M.; Youn, S.J.; Choi, Y.; Lee, N.Y.; Oh, H.J.; Kwon, H.S.; Shin, S.M. Anti-Wrinkle and Skin Moisture Efficacy of 7-MEGA™: A Randomized, Double-Blind, Placebo Comparative Clinical Trial. *Nutrients* **2024**, *16*, 212. [CrossRef]
21. De Souza Pereira, R. Treatment of resistant acne vulgaris in adolescents using dietary supplementation with magnesium, phosphate and fatty acids (omega-6 and omega-7): Comparison with 13-cis-retinoic acid. *J. Diet. Suppl.* **2023**, *20*, 706–716. [CrossRef]
22. Dulf, F.V. Fatty acids in berry lipids of six sea buckthorn (*Hippophae rhamnoides* L. ssp. carpatica) cultivars grown in Romania. *Chem. Cent. J.* **2012**, *6*, 106. [CrossRef] [PubMed]
23. Fatima, T.; Snyder, C.L.; Schroeder, W.R.; Cram, D.; Datla, R.; Wishart, D.; Weselake, R.J.; Krishna, P. Fatty acid composition of developing sea buckthorn (*Hippophae rhamnoides* L.) berry and the transcriptome of the mature seed: Unlocking the value of sea buckthorn for global application in health and nutrition. *BMC Genom.* **2012**, *13*, 353.
24. Aquino-Bolaños, E.N.; Mapel-Velazco, L.; Martin-del-Campo, S.T.; Chávez-Servia, J.L.; Martínez, A.J.; Verdalet-Guzmán, I. Fatty acids profile of oil from nine varieties of macadamia nut. *Int. J. Food Prop.* **2017**, *20*, 1262–1269. [CrossRef]
25. O'Hare, T.J.; Trieu, H.H.; Topp, B.; Russell, D.; Pun, S.; Torrisi, C.; Liu, D. Assessing fatty acid profiles of macadamia nuts. *HortScience* **2019**, *54*, 633–637. [CrossRef]
26. Ren, G.; Yang, B.; Tarkka, M. Sea buckthorn (*Hippophae rhamnoides* L.) oils and their components: A review of composition and bioactivities. *RSC Adv.* **2020**, *10*, 44654–44671. [CrossRef]
27. Vilas-Franquesa, A.; Saldo, J.; Juan, B. Potential of sea buckthorn-based ingredients for the food and feed industry—A review. *Food Prod. Process. Nutr.* **2020**, *2*, 17. [CrossRef]
28. Ojha, P.K.; Poudel, D.K.; Rokaya, A.; Maharjan, S.; Timsina, S.; Poudel, A.; Satyal, R.; Satyal, P.; Setzer, W.N. Chemical compositions and essential fatty acid analysis of selected vegetable oils and fats. *Compounds* **2024**, *4*, 37–70. [CrossRef]

29. Zhou, Y.; Sun, M.L.; Lin, L.; Ledesma-Amaro, R.; Wang, K.; Ji, X.J.; Huang, H. Dynamic regulation combined with systematic metabolic engineering for high-level palmitoleic acid accumulation in oleaginous yeast. *Metab. Eng.* **2025**, *89*, 33–46. [CrossRef]
30. Li, S.; Lei, H.; Li, W.; Bai, Y.; Li, J.; Liu, Y. Overproduction of palmitoleic acid by engineering and process optimization in *Saccharomyces cerevisiae*. *Bioresour. Technol.* **2023**, *382*, 129211. [CrossRef] [PubMed]
31. Kamisaka, Y.; Kimura, K.; Uemura, H.; Yamaoka, M. Addition of methionine and low cultivation temperatures increase palmitoleic acid production by engineered *Saccharomyces cerevisiae*. *Appl. Microbiol. Biotechnol.* **2015**, *99*, 201–210. [CrossRef] [PubMed]
32. Qian, X.; Lei, H.; Zhou, X.; Zhang, L.; Cui, W.; Zhou, J.; Xin, F.; Dong, W.; Jiang, M.; Ochsenreither, K. Engineering *Scheffersomyces segobiensis* for palmitoleic acid-rich lipid production. *Microb. Biotechnol.* **2024**, *17*, e14301. [CrossRef]
33. Park, W.S.; Shin, K.S.; Jung, H.W.; Lee, Y.; Sathesh-Prabu, C.; Lee, S.K. Combinatorial metabolic engineering for secretory production of free fatty acids with high unsaturated fatty acids in *Escherichia coli*. *J. Agric. Food Chem.* **2022**, *70*, 13913–13921. [CrossRef]
34. Kobalter, S.; Voit, A.; Bekerle-Bogner, M.; Rudalija, H.; Haas, A.; Wriessnegger, T.; Pichler, H. Tuning fatty acid profile and yield in Pichia pastoris. *Bioengineering* **2023**, *10*, 1412. [CrossRef]
35. Kolouchová, I.; Schreiberová, O. Biotransformation of volatile fatty acids by oleaginous and non-oleaginous yeast species. *FEMS Yeast Res.* **2015**, *15*, fov076. [CrossRef]
36. Parker, L.; Ward, K.; Pilarski, T.; Price, J.; Derkach, P.; Correa, M.; Miller, R.; Benites, V.; Athanasiadis, D.; Doherty, B.; et al. Development and large-scale production of high-oleic acid oil by fermentation of microalgae. *Fermentation* **2024**, *10*, 566. [CrossRef]
37. *CA3039432A1*; Tailored Oils Produced from Recombinant Heterotrophic Microorganisms. Corbion Biotech Inc.: Lenexa, KS, USA, 2011.
38. Christie, W.W.; Robertson, G.W.; McRoberts, W.C.; Hamilton, J.G. Mass spectrometry of the 4,4-dimethyloxazoline derivatives of isomeric octadecenoates (monoenes). *Eur. J. Lipid Sci. Technol.* **2000**, *102*, 23–29. [CrossRef]
39. Zhang, J.Y.; Yu, Q.T.; Liu, B.N.; Huang, Z.H. Chemical modification in mass spectrometry. IV. 2-Alkenyl-4,4-dimethyloxazolines as derivatives for the double bond location of long-chain olefinic acids. *Biomed. Environ. Mass. Spectrom.* **1988**, *15*, 33–44. [CrossRef]
40. Zhou, X.; Zhou, D.; Bao, X.; Zhang, Y.; Zhou, J.; Xin, F.; Zhang, W.; Qian, X.; Dong, W.; Jiang, M.; et al. Production of palmitoleic acid by oleaginous yeast *Scheffersomyces segobiensis* DSM 27193 using systematic dissolved oxygen regulation strategy. *Chin. J. Chem. Eng.* **2023**, *53*, 324–331. [CrossRef]
41. Gluth, A.; Trejo, J.B.; Czaijka, J.J.; Deng, S.; Qian, W.J.; Yang, B.; Zhang, T. Proteomics insights into the physiology and metabolism of oleaginous yeasts and filamentous fungi. *Front. Microbiol.* **2025**, *16*, 1637123. [CrossRef] [PubMed]
42. Yu, T.; Zhou, Y.J.; Huang, M.; Liu, Q.; Pereira, R.; David, F.; Nielsen, J. Reprogramming yeast metabolism from alcoholic fermentation to lipogenesis. *Cell* **2018**, *174*, 1549–1558.e14. [CrossRef] [PubMed]
43. Cai, P.; Wu, X.; Deng, J.; Gao, L.; Shen, Y.; Yao, L.; Zhou, Y.J. Methanol biotransformation toward high-level production of fatty acid derivatives by engineering the industrial yeast *Pichia pastoris*. *Proc. Natl. Acad. Sci. USA* **2022**, *119*, e2201711119. [CrossRef]
44. Xiao, K.; Yue, X.H.; Chen, W.C.; Zhou, X.R.; Wang, L.; Xu, L.; Huang, F.H.; Wan, X. Metabolic engineering for enhanced medium chain omega hydroxy fatty acid production in *Escherichia coli*. *Front. Microbiol.* **2018**, *9*, 139. [CrossRef] [PubMed]